in vivo *36*: 2790-2799 (2022)
doi:10.21873/invivo.13016

Differentiation of Angiomyolipoma With Minimal Fat from Clear Cell Renal Cell Carcinoma Using Non-contrast Multiparametric Magnetic Resonance Imaging

WATARU JOMOTO[1,2], HARUYUKI TAKAKI[1], SHINGO YAMAMOTO[3], AKIHIRO KANEMATSU[3], MASATAKA IGETA[4], SEIICHI HIROTA[5] and KOICHIRO YAMAKADO[1]

[1]*Department of Radiology, Hyogo Medical University, Nishinomiya, Japan;*
[2]*Department of Radiological Technology, Hyogo Medical University Hospital, Nishinomiya, Japan;*
[3]*Department of Urology, Hyogo Medical University, Nishinomiya, Japan;*
[4]*Department of Biostatistics, Hyogo Medical University, Nishinomiya, Japan;*
[5]*Department of Surgical Pathology, Hyogo Medical University, Nishinomiya, Japan*

Abstract. *Background/Aim: This study was conducted to ascertain the optimal combination of non-contrast magnetic resonance (MR) imaging sequences for the differential diagnosis between small angiomyolipoma (AML) with minimal fat and clear cell renal cell carcinoma (CCRCC). Patients and Methods: Thirty-nine patients with pathologically proven AML with minimal fat (n=6) or CCRCC (n=33) measuring 4 cm or less were included. All underwent MR imaging before partial nephrectomy or percutaneous biopsy. Four quantitative parameters of tumors were evaluated: signal intensity (SI) index of T1W- gradient-echo imaging, SI index of T2- fat suppression imaging (T2-SI index), apparent diffusion coefficient (ADC) value, and standard deviation (SD) of ADC. These quantitative parameters were compared using Wilcoxon rank-sum test and receiver operating characteristic (ROC) curve analyses. The optimal combination of quantitative parameters was sought using logistic regression analysis. Results: Comparison of quantitative parameters showed that the T2-SI index (median, AML with minimal fat vs. CCRCC; 0.74 vs. 1.27, p<0.001), ADC value (1.12 vs. 1.75, p=0.005), and SD of ADC (104 vs. 233, p<0.001) were significantly lower in AML with minimal fat than CCRCC. From the ROC curve analysis, the highest area under the curve (1.000; 100% sensitivity; 100% specificity) was obtained using the logistic regression model with the SD of ADC and T2-SI index or ADC value as explanatory variables. Conclusion: SD of ADC combined with T2-SI index or ADC value exhibited the highest diagnostic performance for differentiating small AML with minimal fat from CCRCC.*

Correspondence to: Haruyuki Takaki, MD, Ph.D., Department of Radiology, Hyogo Medical University, 1-1 Mukogawa-cho, Nishinomiya City, Hyogo Prefecture, 663-8501 Japan. Tel: +81 798456362, Fax: +81 798456361, e-mail: takakiharuyuki@gmail.com

Key Words: Angiomyolipoma with minimal fat, clear cell renal cell carcinoma, magnetic resonance imaging, prediction model, apparent diffusion coefficient.

This article is an open access article distributed under the terms and conditions of the Creative Commons Attribution (CC BY-NC-ND) 4.0 international license (https://creativecommons.org/licenses/by-nc-nd/4.0).

The number of incidentally detected small renal tumors is increasing because of the widespread use of various imaging methods such as computed tomography (CT) and magnetic resonance (MR) imaging (1, 2). Of these incidentally detected small renal tumors, 12-16% are reported as benign renal tumors (3, 4). Angiomyolipoma (AML), the most common benign renal tumor, accounts for 43-75% of all resected benign renal tumors (3-6).

The diagnosis of AML can be reached easily if macroscopic fat is observed within the renal tumor on CT or MR imaging (7, 8). However, of all AMLs, approximately 5% have low fat content, designated as AML with minimal fat (9). Both AML with minimal fat and clear cell renal cell carcinoma (CCRCC) are shown by dynamic CT or MR imaging as hypervascular tumors (10). Therefore, differential diagnosis between AML with minimal fat and CCRCC is difficult to accomplish using dynamic CT or MR imaging. Invasive diagnostic methods such as percutaneous needle biopsy and surgical resection are necessary.

Several studies have been conducted to establish non-invasive differential diagnosis between AML with minimal fat and CCRCC using non-contrast MR imaging (6). Choi *et al.* reported that AML with minimal fat showed a significantly

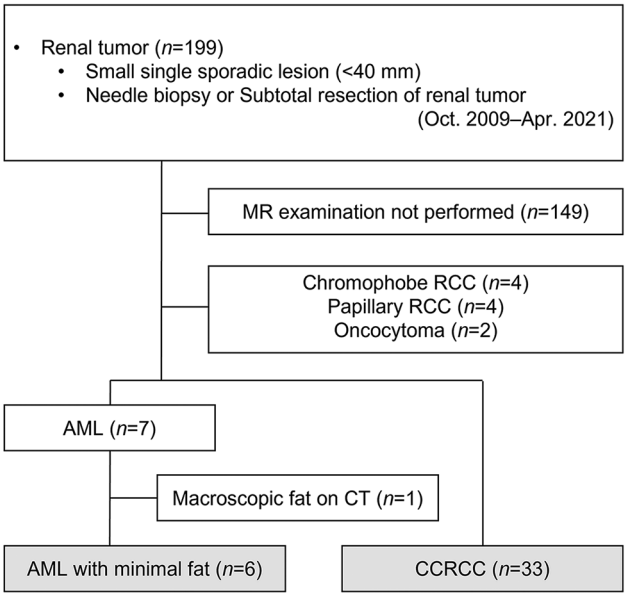

Figure 1. *Study flowchart shows patient inclusion and exclusion criteria and final diagnosis. MR: Magnetic resonance; RCC: renal cell carcinoma; AML: angiomyolipoma; CCRCC: clear cell renal cell carcinoma; CT: computed tomography.*

lower tumor to spleen signal intensity (SI) ratio on T2-weighted images than that shown by renal cell carcinoma (RCC) (11). Park *et al*. reported the apparent diffusion coefficient (ADC) is significantly lower in RCC than in AML with minimal fat (12). These studies examined a specific MR imaging sequence. If a combination of multiple sequences is used, then the accuracy of differential diagnosis between AML with minimal fat and RCC might improve. Nevertheless, few reports to date have described such an approach (13).

This study was conducted to ascertain the optimum combination of non-contrast MR imaging sequences for differential diagnosis between AML with minimal fat and CCRCC.

Patients and Methods

Patients. This retrospective study, which was approved by our institutional review board (approval number: 202112-039), was conducted in accordance with the ethical standards of the Declaration of Helsinki. The requirement for informed consent was waived.

From October 2009 through April 2021, 199 patients underwent partial nephrectomy (*n*=118), percutaneous biopsy (*n*=79), or both nephrectomy and biopsy (*n*=2) for renal tumors that were 4 cm or smaller. Of these, 50 patients underwent renal MR imaging examination within 2 months before partial nephrectomy or biopsy. The histological diagnoses of renal tumors in these 50 patients were CCRCC (*n*=33), AML (*n*=7), chromophobe RCC (*n*=4), papillary RCC (*n*=4), and oncocytoma (*n*=2). From them, 10 patients with chromophobe RCC, papillary RCC, and oncocytoma were excluded.

Table I. *Clinical characteristics*.

	AML with minimal fat (n=6)	CCRCC (n=33)	*p*-Value
Demographics			
Sex			<0.01
Male	0 (0)	24 (73)	
Female	6 (100)	9 (27)	
Age	52.0	61.0	0.24
(years)	(42.5-62.8)	(49.0-70.0)	
Tumor			
Side (right/left)			0.18
Right	4 (67)	11 (33)	
Left	2 (33)	22 (67)	
Size (mm)	22.5	20.0	0.34
Diagnosis method	(15.3-38.0)	(15.5-25.0)	0.64
Biopsy	2 (33)	8 (24)	
Partial nephrectomy	4 (67)	25 (76)	
Biochemical			
Total protein (g/dl)	7.1 (6.8-7.6)	7.2 (6.8-7.5)	0.74
Aspartate aminotransferase (U/l)	25.0 (19.0-37.3)	22.0 (17.5-29.5)	0.56
Alanine aminotransferase (U/l)	25.0 (16.5-29.5)	27.0 (16.0-40.5)	0.57
Alkali phosphatase (U/l)	118.0 (66.0-232.5)	192.0 (151.5-242.5)	0.14
Estimated glomerular filtration rate (ml/min/1.73 m^2)	82.0 (74.8-122.3)	78.0) (67.0-91.3	0.21
C-reactive protein (mg/ml)	0.05 (0.02-0.09)	0.10 (0.04-0.12)	0.14
Platelet ($\times 10^4$/μl)	22.7 (18.6-23.6)	22.1 (18.9-25.2)	0.88

Continuous data are presented as median (interquartile range). Categorical variables are the number of patients with percentage in parentheses, n (%). *p*-Values were calculated using the Wilcoxon rank-sum test for continuous variables and the Fisher's exact test for categorical variables. AML: Angiomyolipoma; CCRCC: clear cell renal cell carcinoma.

A patient with fat-rich AML in whom macroscopic fat component was identifiable on CT was excluded from this study. Therefore, this study examined 39 patients with AML with minimal fat (*n*=6) and CCRCC (*n*=33) (Figure 1).

Patient characteristics and tumor characteristics are presented in Table I. The proportion of female patients in the AML with minimal fat group was significantly higher than that in the CCRCC group (100% *vs*. 27%, $p<0.01$). All other background characteristics were comparable between the two groups.

MR imaging acquisition protocol. For this study, 25 patients were examined using a 1.5T-MR imaging scanner (MAGNETOM Avant; Siemens Healthineers AG, Erlangen, Germany; or Intera, Philips Healthcare, Best, the Netherlands). Also, 14 patients were examined using a 3.0T-MR imaging scanner (MAGNETOM Skyra; Siemens Healthineers AG, Erlangen, Germany or Ingenia 3.0T; Philips

Healthcare). The receiving coil was a phased array coil for abdominal MR imaging recommended at each scanner. The imaging orientation was set as transverse in all sequences.

The following sequences were obtained: T1 weighted opposed-phase and in-phase gradient-echo imaging (T1-GRE), T2 weighted turbo spin echo with fat suppression imaging (T2-FS), and ADC map generated by spin echo-diffusion weighted image (DWI). Imaging of T1-GRE and T2-FS were obtained with breath-holding; DWI was obtained using respiratory synchronization technology. The 1.5T-MR examinations were performed with the following settings. T1-GRE was obtained as follows: time of repetition (TR), 140-210 ms; echo time (TE), 2.29-2.40 ms (opposed-phase) and 4.64-4.87 ms (in-phase); flip angle, 75-80 degrees; slice thickness, 5-7 mm; field of view (FOV), 270-380 mm and matrix, 256. In addition, T2-FS was obtained as follows: TR, 3,000-3,500 ms; TE, 66-100 ms; refocusing flip angle, 120-180 degree; slice thickness, 5-7 mm; FOV, 270-380 mm and matrix, 256-320. DWI was obtained as follows: TR, breathing interval; TE, 66-75 ms; slice thickness, 5-7 mm; FOV, 270-380 mm; matrix,106-128; b-factor, 0 and 900-1,000 s/mm^2, and ADC created from DWI of the acquired b value. The 3.0T-MR imaging examination was performed as explained hereinafter. The T1-GRE was obtained as follows: TR, 158-313 ms; TE, 1.23-1.39 ms (opposed-phase) and 2.30-2.46 ms (in-phase); flip angle, 70 degrees; slice thickness, 5-6 mm; FOV, 295-350 mm and matrix, 256. In addition, T2-FS was obtained as follows: TR, 3,000-5,050 ms; TE, 66-100 ms; refocusing flip angle, 120-180 degree; slice thickness, 5-6 mm; FOV, 295-350 mm and matrix, 288-320. DWI was obtained as follows: TR, breathing interval; TE, 65-78 ms; slice thickness, 5-6 mm; FOV, 295-350 mm; matrix, 96-128; b-factor, 0 and 900-1,000 s/mm^2, and ADC created from DWI of the acquired b value.

Imaging analysis. Imaging analysis was performed by one abdominal radiologist and one radiological technologist, respectively with 22 and 15 years of experience interpreting genitourinary images. Imaging analyses were performed using an image archiving and communication system (SYNAPSE®; Fujifilm Medical Co., Ltd., Tokyo, Japan). In each sequence, a slice image for analysis was chosen at the maximum renal tumor size. Subsequently, a region of interest (ROI) was assigned for the tumor. An analysis was performed. The size of each ROI comprised about 80% of the target tumor.

For this study, the SI index of T1W-GRE (T1-SI index), SI index of T2-FS (T2-SI index), ADC value, and standard deviation (SD) of ADC were evaluated. The T1-SI index was calculated using the following equation: T1-SI index=$(SI_{in}-SI_{opp})/SI_{in}$ where SI_{in} and SI_{opp} respectively denote the tumor signal intensity on opposed-phase and in-phase images. The T2-SI index was calculated as T2-SI index=SI_t/SI_c, where SI_t and SI_c, respectively, denote the signal intensity with tumor and renal cortex in T2-FS. The ADC value and SD of ADC were obtained from the ROI in the ADC map.

Statistical analysis. For summarizing patient characteristics and quantitative parameters from imaging analysis of renal tumors, the median and interquartile range (IQR) were used as continuous variables. A frequency distribution is shown for categorical variables. The Wilcoxon rank-sum test for continuous variables and the Fisher's exact test for categorical variables were used to calculate *p*-values for comparison between the AML with minimal fat group and the CCRCC group.

Table II. *Comparisons of quantitative parameters between renal tumors*.

Parameter	AML with minimal fat (n=6)	CCRCC (n=33)	*p*-Value
DT1-SI index	0.10 (0.06-0.29)	0.07 (0.00-0.30)	0.521
T2-SI index	0.74 (0.62-0.79)	1.27 (1.10-1.41)	<0.001
ADC value ($\times10^{-3}$mm^2/s)	1.12 (0.83-1.38)	1.75 (1.33-2.00)	0.005
SD of ADC	104 (99.2-144)	233 (187-331)	<0.001

Continuous data are presented as median (interquartile range). *p*-Values were calculated using the Wilcoxon rank-sum test. AML: Angiomyolipoma; CCRCC: clear cell renal cell carcinoma; T1-SI index: signal intensity index of T1 weighted opposed and in phase gradient-echo imaging; T2-SI index: signal intensity of T2 weighted turbo spin echo with fat suppression imaging; ADC: apparent diffusion coefficient; SD: standard deviation.

Receiver operating characteristic (ROC) analysis was performed for each quantitative parameter used in the image analysis of renal tumors. The area under the curve (AUC) and the cutoff threshold of each quantitative parameter that maximizes the Youden index were estimated. The sensitivity and specificity were calculated under the estimated cutoff threshold. For differential diagnoses of AML with minimal fat from CCRCC, the combination of quantitative parameters that maximizes the Youden index was estimated *via* the logistic regression analysis with the differential diagnosis result of AML with minimal fat from CCRCC as the response variable and two of the four quantitative parameters (T1-SI index, T2-SI index, ADC value, and SD of ADC) in image analysis as the explanatory variables. For complete separation, the parameters were estimated using Firth's bias correction method (14). Based on the estimated logistic regression model, the AUC and cutoff threshold for the probability of AML with minimal fat that maximizes the Youden index were estimated. The sensitivity and specificity were calculated under the cutoff threshold. Models for differentiation between small AML with minimal fat and CCRCC on non-contrast MR imaging are shown with the threshold for the linear predictor of the logistic regression model, as obtained by back-calculation of the threshold for the probability of AML with minimal fat.

Results with a two-sided *p*-value <0.05 were inferred as statistically significant without adjustment of multiplicity. All analyses were performed using JMP Pro 15 and SAS software ver. 9.4 (SAS Institute Inc., Cary, NC, USA).

Histopathological observation. After the threshold value for the linear combination of the two selected quantitative parameters was obtained, histopathology of CCRCC, which was closest to the threshold value of the prediction model, was observed. The histopathologies of AML with minimal fat and CCRCC that were separated from the threshold value of the prediction model were also observed.

Results

Comparisons of quantitative parameters. Table II presents values of AML with minimal fat and CCRCC groups for the quantitative parameters. The T2-SI index [median (IQR) of

Table III. *Diagnostic performance of each quantitative parameter.*

Parameter	AUC	Cutoff for parameter	Sensitivity (%)	Specificity (%)	Youden index
T1-SI index	0.586	0.067	83.3	51.5	0.349
T2-SI index	0.939	0.818	100.0	90.9	0.909
ADC value	0.871	1.468	100.0	66.7	0.667
SD of ADC	0.970	141.000	83.3	100.0	0.833

AUC: Area under the curve; T1-SI index: signal intensity index of T1 weighted opposed and in phase gradient-echo imaging; T2-SI index: signal intensity of T2 weighted turbo spin echo with fat suppression imaging; ADC: apparent diffusion coefficient; SD: standard deviation.

Table IV. *Logistic prediction model for the differential diagnosis of angiomyolipoma (AML) with minimal fat and clear cell renal cell carcinoma (CCRCC) by combination of two parameters.*

Parameter	AUC	Linear predictor	Cutoff for linear predictor	Sensitivity (%)	Specificity (%)
T1-SI index and T2-SI index	0.949	–0.50546*(T1-SI index)-9.80464*(T2-SI index)	–8.14859	100	90.9
T1-SI index and ADC value	0.869	–0.08427*(T1-SI index)-5.47931*(ADC value)	–7.64647	100	69.7
T1-SI index and SD of ADC	0.970	2.84045*(T1-SI index)-0.08019*(SD of ADC)	–12.10159	100	87.9
T2-SI index and ADC value	0.944	–8.48704*(T2-SI index)-0.94543*(ADC value)	–8.25727	100	90.9
T2-SI index and SD of ADC	1.000	–5.84427*(T2-SI index)-0.02605*(SD of ADC)	–9.00146	100	100.0
ADC value and SD of ADC	1.000	–3.84067*(ADC value)-0.03709*(SD of ADC)	–10.89482	100	100.0

AUC: Area under the curve; T1-SI index: signal intensity index of T1 weighted opposed and in phase gradient-echo imaging; T2-SI index: signal intensity of T2 weighted turbo spin echo with fat suppression imaging; ADC: apparent diffusion coefficient; SD: standard deviation.

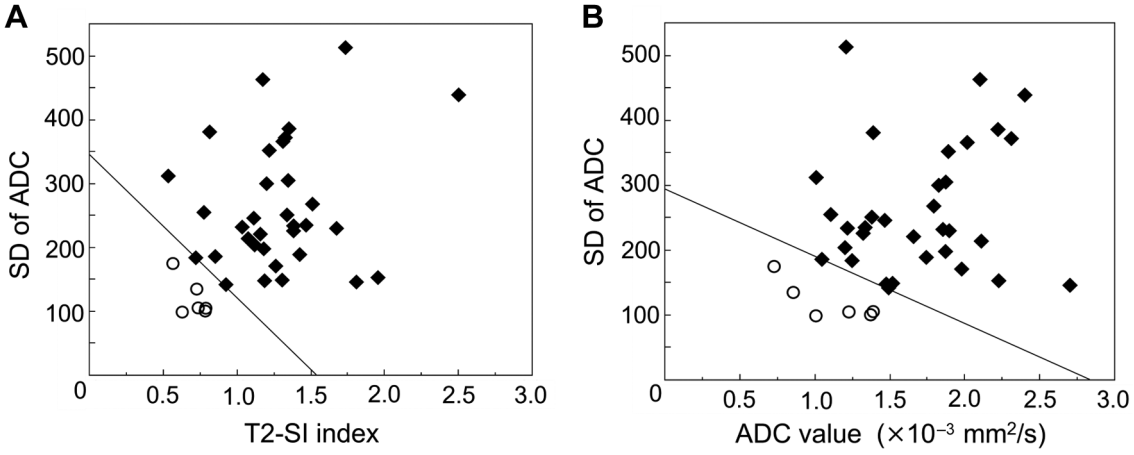

Figure 2. *Scatter plots between the standard deviation (SD) of apparent diffusion coefficient (ADC) and T2-signal intensity (SI) or ADC value with white circles representing angiomyolipoma (AML) with minimal fat, and black diamonds denoting clear cell renal cell carcinoma (CCRCC). The solid line represents the threshold for the linear predictor of the logistic regression model with SD of ADC and SI index of T2- fat suppression imaging (T2-SI index) (A) or ADC value (B) as explanatory variables. The combination of SD of ADC and T2-SI index or ADC value completely separated AML with minimal fat and CCRCC by the prediction model.*

AML with minimal fat *vs*. median (IQR) of CCRCC; 0.74 (0.62-0.79) *vs*. 1.27 (1.10-1.41), $p<0.001$], ADC value [1.12 (0.83-1.38) *vs*. 1.75 (1.33-2.00), $p=0.005$] and SD of ADC [104 (99.2-144) *vs*. 233 (187-331), $p<0.001$] were significantly lower for AML with minimal fat than those for CCRCC. No significant difference was found for the T1-SI index [0.10 (0.06-0.29) *vs*. 0.07 (0.00-0.30), $p=0.521$].

Diagnostic performance of each quantitative parameter. The ROC curve analysis showed that the AUC was highest in SD

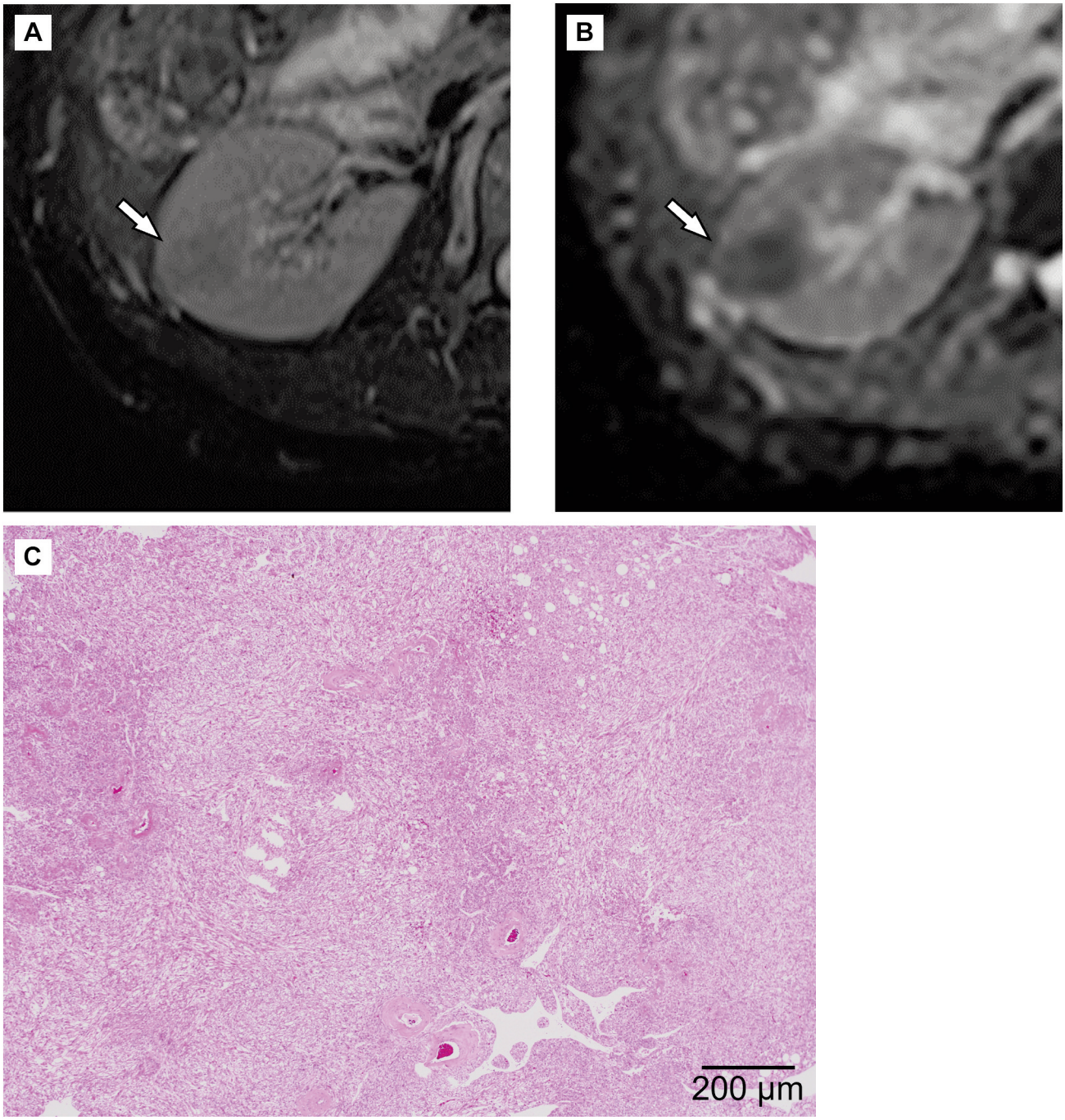

Figure 3. *Images from a 49-year-old woman with right angiomyolipoma (AML) with minimal fat and a 17 mm diameter. (A) The tumor showed a lower signal than that of the renal cortex in T2 weight image with fat suppression (white arrow) and SI index of T2- fat suppression imaging (T2-SI index) was 0.79. (B) The mean apparent diffusion coefficient (ADC) value of the tumor (white arrow) was 1.23×10^{-3} mm^2/s, and standard deviation of ADC was 104. (C) Pathological image of the resected tumor was filled with spindled smooth muscle and micro fat cells.*

of ADC (0.970), followed by the T2-SI index (0.939), ADC value (0.871), and T1-SI index (0.586) (Table III). The sensitivity was 100% in both the T2-SI index and ADC value. The specificity was 100% in SD of ADC.

Diagnostic performance for combinations of quantitative parameters. The logistic prediction model with SD of ADC, and T2-SI index or ADC value achieved the best diagnostic performance (AUC, 1.000; 100% sensitivity; 100% specificity)

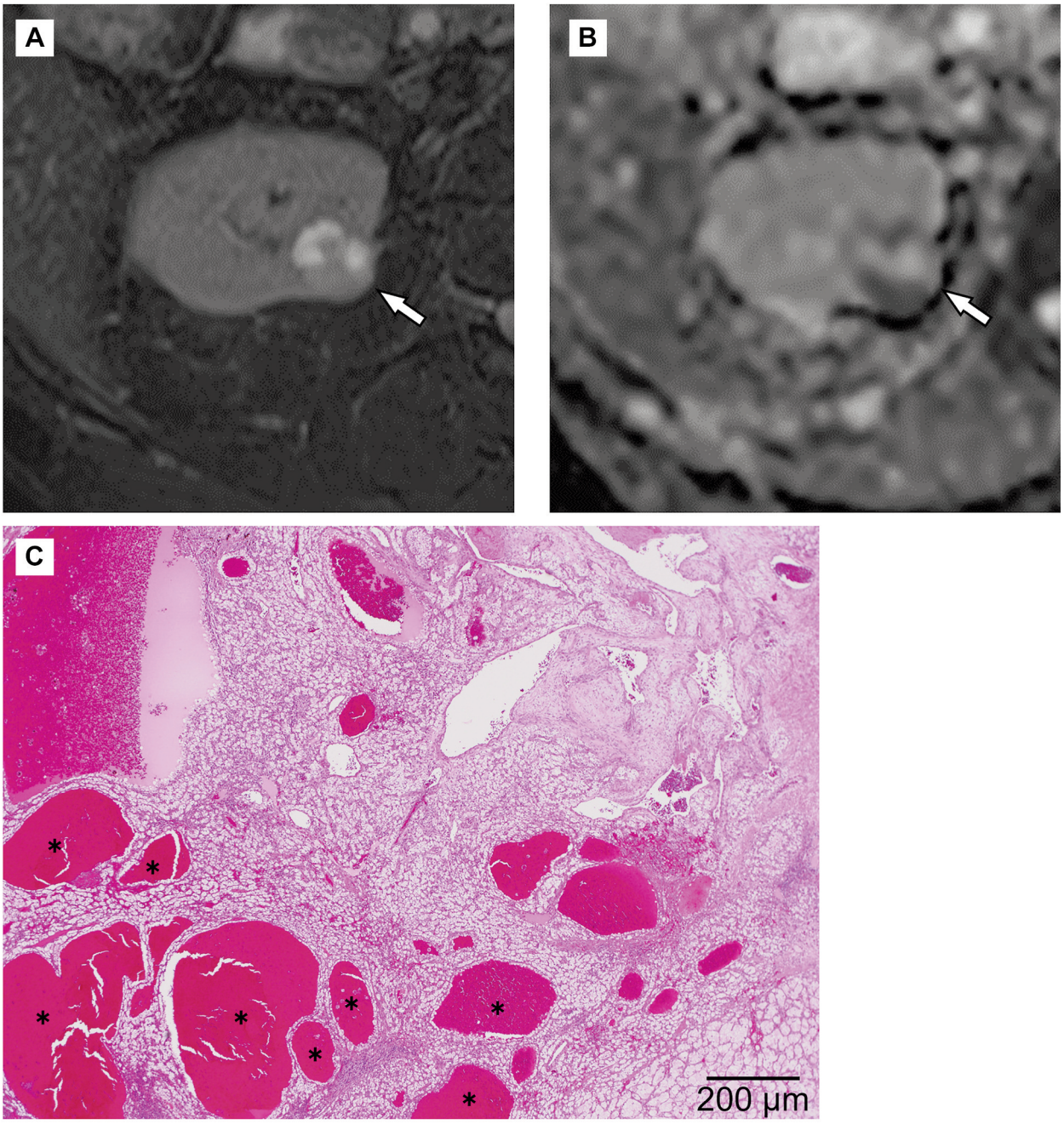

Figure 4. *A 76-year-old woman with right clear cell renal cell carcinoma with a 19 mm diameter. (A) The tumor shows heterogeneous hyperintensity at T2 weight image with fat suppression compared to the renal cortex (white arrow). The SI index of T2- fat suppression imaging (T2-SI index) was 1.73. (B) The mean apparent diffusion coefficient (ADC) value of tumor (white arrow) was 1.21×10^{-3} mm^2/s. The standard deviation (SD) of ADC was 512. (C) A pathology image of the resected tumor indicated noticeable atypical cells, necrosis, and bleeding (asterisk). This case was far from the predictive model with the combination of SD of ADC and T2-SI index. The SD of ADC was the highest in this study.*

for differentiation between small AML with minimal fat and CCRCC (Table IV, Figure 2).

Histopathological observation. The histopathology of AML with minimal fat, separated from the threshold value of the linear predictor of the logistics regression model with SD of ADC and T2-SI index, mainly comprised spindled smooth muscle cells with a small amount of fat, and an abnormally thick-walled blood vessel component (Figure 3). Neither intratumoral hemorrhage nor necrosis was observed. CCRCC

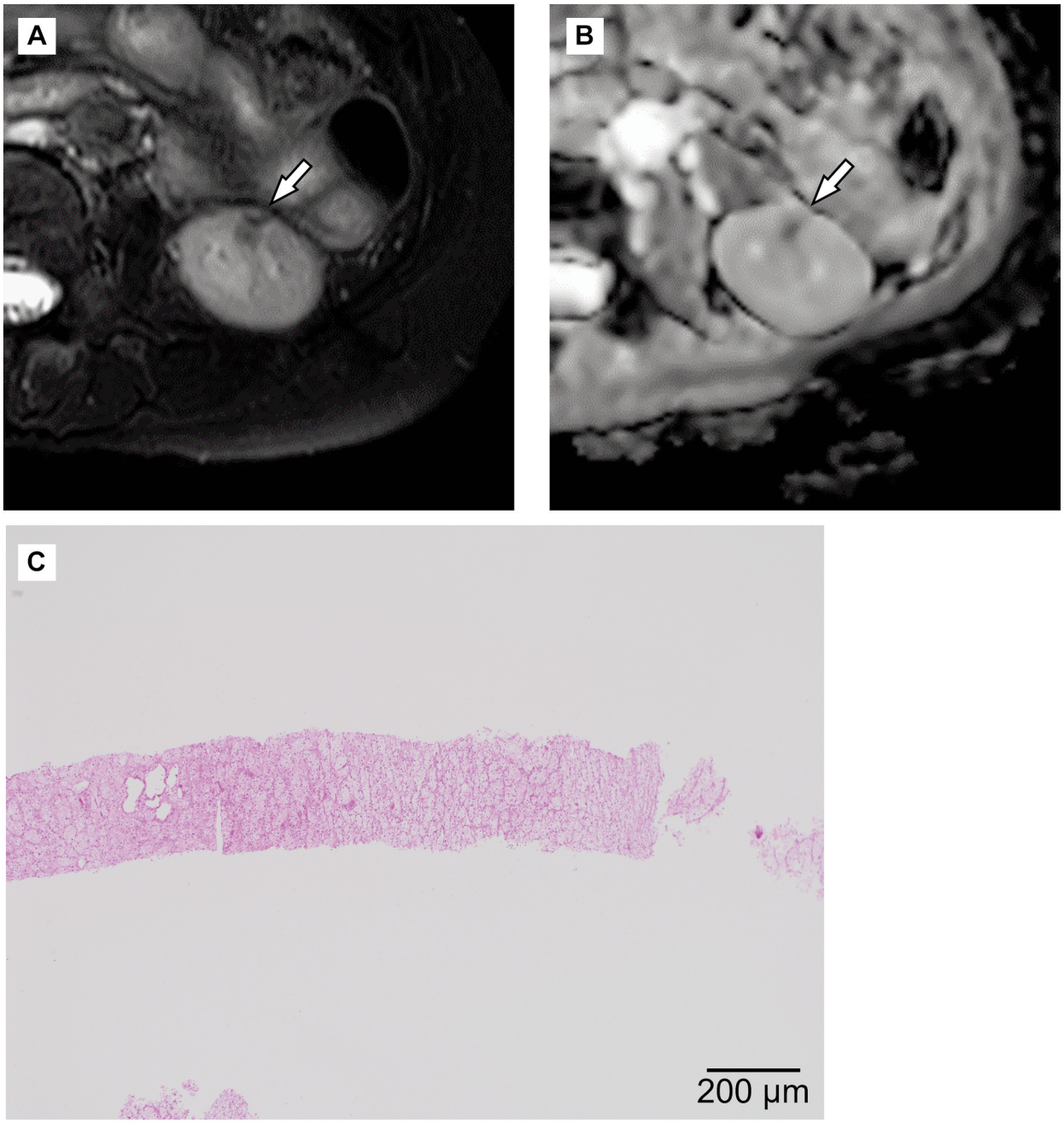

Figure 5. *A 54-year-old woman with left clear cell renal cell carcinoma with an 8 mm diameter. This patient is close to the prediction model in the combination of standard deviation (SD) of apparent diffusion coefficient (ADC) and SI index of T2- fat suppression imaging (T2-SI index). (A) Tumor showed a low signal in the T2 weight image with fat suppression (white arrow); the T2-SI index was 0.72. (B) Mean ADC value of tumor (white arrow) was 1.25×10^{-3} mm^2/s, and SD of ADC was 183. (C)Pathological image obtained by biopsy post radiofrequency ablation therapy. Adipose tissue is observed, but there is no bleeding or necrosis.*

separated from the threshold value included intratumoral hemorrhage and necrosis (Figure 4). However, the CCRCC that was closest to the threshold value of the prediction model included no intratumoral hemorrhage or necrosis within the observable range (Figure 5 and Figure 6).

Discussion

Results of this study indicated SD of ADC, T2-SI index, and ADC value as useful for differentiating small AML with minimal fat from CCRCC. Furthermore, the diagnostic

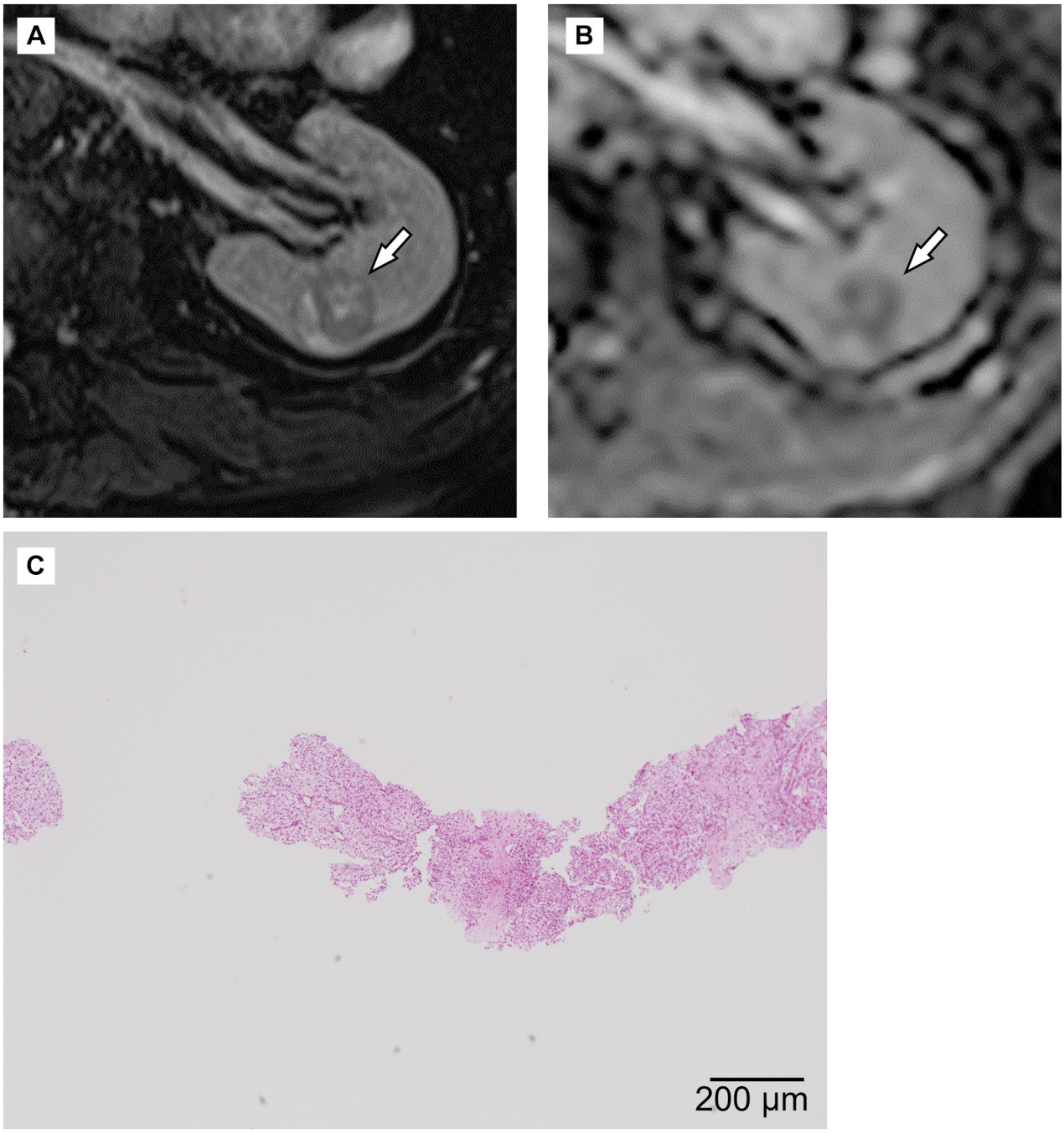

Figure 6. *A 75-year-old man with left clear cell renal cell carcinoma with a 20 mm diameter. This patient was close to the prediction model in the combination of standard deviation (SD) of apparent diffusion coefficient (ADC) and SI index of T2- fat suppression imaging (T2-SI index). (A) The tumor showed a mixture of low and high signals in T2 weight image with fat suppression T2-FS (white arrow) and T2-SI index was 0.93. (B) The mean ADC value of the tumor (white arrow) was 1.49×10^{-3} mm^2/s. The SD of ADC was 141. (C) Pathological image obtained by biopsy before cryotherapy. No finding was suggestive of bleeding or necrosis in the image.*

performance improved further when the SD of ADC and T2-SI index or ADC value were combined.

In fact, AML with minimal fat is known to show a lower T2-SI index because the tumor predominantly comprises smooth muscle cells (5, 15, 16). Sasiwimonphan *et al.* reported that AML with minimal fat can be differentiated from RCC with high sensitivity if using a threshold T2-SI index of 0.9 (17). Data of this study support results reported

by Sasiwimonphan *et al*. For this study, the median T2-SI index of AML with minimal fat was 0.74 (IQR=0.62-0.79), whereas CCRCC was 1.27 (IQR=1.10-1.41).

This study revealed the ADC value of AML with minimal fat as significantly lower than that of CCRCC. Moreover, the SD of ADC was significantly lower in AML with minimal fat than that of CCRCC. Similar results were reported by Li *et al*., who described that the mean ADC value and SD of ADC in CCRCC were significantly higher than those of AML with minimal fat (18). These differences are most likely attributable to differences in their components. Histopathological analysis undertaken for this study showed that AML with minimal fat had uniform proliferation of smooth muscle cells, whereas intratumoral hemorrhage and necrosis were observed in CCRCC. Moreover, the ADC value and SD of ADC of CCRCC with less intratumoral hemorrhage and necrosis were close to those of AML with minimal fat. These results suggest that intratumoral hemorrhage and necrosis contributes to the increase in the ADC value and SD of ADC in CCRCC (19).

It is noteworthy that the differentiation of small AML with minimal fat and CCRCC with higher sensitivity and specificity became possible by combining two parameters: SD of ADC, and the T2-SI index or ADC value. An approach that can ascertain a threshold for linear combinations based on logistic regression and which can develop a predictive model, as used for this study, can be expected to contribute to higher diagnostic performance for differentiating small AML with minimal fat from CCRCC.

This study has several limitations including the small number of patients, retrospective study design, and biased patients' backgrounds. Therefore, the results of this study must be validated using a prospective study conducted with a greater number of patients. In addition, multiple MR imaging scanners and different magnetic field strengths (*i.e*., 1.5-T and 3.0-T) were used for this study. Therefore, prediction models and threshold values obtained from this study are inapplicable to different MR scanners.

In conclusion, combinations of SD of ADC with the T2-SI index or ADC value provided high diagnostic performance for differentiation between small AML with minimal fat and CCRCC.

Conflicts of Interest

The Authors declare that they have no conflicts of interest in relation to this study.

Authors' Contributions

W.J. was involved in the methodology, investigation, data curation and writing-original draft. H.T. was involved in the conceptualization, methodology, formal analysis, writing-review & editing and project administration supervision. S.Y. and A.K. were involved in the conceptualization and formal analysis. M.I. was involved in methodology and formal analysis. S.H. was involved in the formal analysis. K.Y. was involved in the supervision. All Authors critically revised the manuscript, approved it for publication, and agreed to accept responsibility for all aspects.

References

1 Silverman SG, Israel GM, Herts BR and Richie JP: Management of the incidental renal mass. Radiology *249(1)*: 16-31, 2008. PMID: 18796665. DOI: 10.1148/radiol.2491070783

2 Volpe A, Panzarella T, Rendon RA, Haider MA, Kondylis FI and Jewett MA: The natural history of incidentally detected small renal masses. Cancer *100(4)*: 738-745, 2004. PMID: 14770429. DOI: 10.1002/cncr.20025

3 Fujii Y, Komai Y, Saito K, Iimura Y, Yonese J, Kawakami S, Ishikawa Y, Kumagai J, Kihara K and Fukui I: Incidence of benign pathologic lesions at partial nephrectomy for presumed RCC renal masses: Japanese dual-center experience with 176 consecutive patients. Urology *72(3)*: 598-602, 2008. PMID: 18649929. DOI: 10.1016/j.urology.2008.04.054

4 Kutikov A, Fossett LK, Ramchandani P, Tomaszewski JE, Siegelman ES, Banner MP, Van Arsdalen KN, Wein AJ and Malkowicz SB: Incidence of benign pathologic findings at partial nephrectomy for solitary renal mass presumed to be renal cell carcinoma on preoperative imaging. Urology *68(4)*: 737-740, 2006. PMID: 17070344. DOI: 10.1016/j.urology.2006.04.011

5 Jinzaki M, Silverman SG, Akita H, Nagashima Y, Mikami S and Oya M: Renal angiomyolipoma: a radiological classification and update on recent developments in diagnosis and management. Abdom Imaging *39(3)*: 588-604, 2014. PMID: 24504542. DOI: 10.1007/s00261-014-0083-3

6 Lopes Vendrami C, Parada Villavicencio C, DeJulio TJ, Chatterjee A, Casalino DD, Horowitz JM, Oberlin DT, Yang GY, Nikolaidis P and Miller FH: Differentiation of solid renal tumors with multiparametric MR imaging. Radiographics *37(7)*: 2026-2042, 2017. PMID: 29131770. DOI: 10.1148/rg.2017170039

7 Halpenny D, Snow A, McNeill G and Torreggiani WC: The radiological diagnosis and treatment of renal angiomyolipoma-current status. Clin Radiol *65(2)*: 99-108, 2010. PMID: 20103431. DOI: 10.1016/j.crad.2009.09.014

8 Bosniak MA, Megibow AJ, Hulnick DH, Horii S and Raghavendra BN: CT diagnosis of renal angiomyolipoma: the importance of detecting small amounts of fat. AJR Am J Roentgenol *151(3)*: 497-501, 1988. PMID: 3044036. DOI: 10.2214/ajr.151.3.497

9 Jinzaki M, Tanimoto A, Narimatsu Y, Ohkuma K, Kurata T, Shinmoto H, Hiramatsu K, Mukai M and Murai M: Angiomyolipoma: imaging findings in lesions with minimal fat. Radiology *205(2)*: 497-502, 1997. PMID: 9356635. DOI: 10.1148/radiology.205.2.9356635

10 Takahashi N, Leng S, Kitajima K, Gomez-Cardona D, Thapa P, Carter RE, Leibovich BC, Sasiwimonphan K, Sasaguri K and Kawashima A: Small (<4 cm) renal masses: Differentiation of angiomyolipoma without visible fat from renal cell carcinoma using unenhanced and contrast-enhanced CT. AJR Am J Roentgenol *205(6)*: 1194-1202, 2015. PMID: 26587925. DOI: 10.2214/AJR.14.14183

11 Choi HJ, Kim JK, Ahn H, Kim CS, Kim MH and Cho KS: Value of T2-weighted MR imaging in differentiating low-fat renal

angiomyolipomas from other renal tumors. Acta Radiol *52(3)*: 349-353, 2011. PMID: 21498374. DOI: 10.1258/ar.2010.090491

12 Park JJ and Kim CK: Small (<4 cm) renal tumors with predominantly low signal intensity on T2-weighted images: Differentiation of minimal-fat angiomyolipoma from renal cell carcinoma. AJR Am J Roentgenol *208(1)*: 124-130, 2017. PMID: 27824487. DOI: 10.2214/AJR.16.16102

13 Wang W, Cao K, Jin S, Zhu X, Ding J and Peng W: Differentiation of renal cell carcinoma subtypes through MRI-based radiomics analysis. Eur Radiol *30(10)*: 5738-5747, 2020. PMID: 32367419. DOI: 10.1007/s00330-020-06896-5

14 Firth D: Bias reduction of maximum likelihood estimates. Biometrika *80(1)*: 27-38, 2017. DOI: 10.1093/biomet/80.1.27

15 Hafron J, Fogarty JD, Hoenig DM, Li M, Berkenblit R and Ghavamian R: Imaging characteristics of minimal fat renal angiomyolipoma with histologic correlations. Urology *66(6)*: 1155-1159, 2005. PMID: 16360431. DOI: 10.1016/j.urology.2005.06.119

16 Hindman N, Ngo L, Genega EM, Melamed J, Wei J, Braza JM, Rofsky NM and Pedrosa I: Angiomyolipoma with minimal fat: can it be differentiated from clear cell renal cell carcinoma by using standard MR techniques? Radiology *265(2)*: 468-477, 2012. PMID: 23012463. DOI: 10.1148/radiol.12112087

17 Sasiwimonphan K, Takahashi N, Leibovich BC, Carter RE, Atwell TD and Kawashima A: Small (<4 cm) renal mass: differentiation of angiomyolipoma without visible fat from renal cell carcinoma utilizing MR imaging. Radiology *263(1)*: 160-168, 2012. PMID: 22344404. DOI: 10.1148/radiol.12111205

18 Li A, Xing W, Li H, Hu Y, Hu D, Li Z and Kamel IR: Subtype differentiation of small (≤4 cm) solid renal mass using volumetric histogram analysis of DWI at 3-T MRI. AJR Am J Roentgenol *211(3)*: 614-623, 2018. PMID: 29812980. DOI: 10.2214/AJR.17.19278

19 Zhang YD, Wu CJ, Wang Q, Zhang J, Wang XN, Liu XS and Shi HB: Comparison of utility of histogram apparent diffusion coefficient and R2* for differentiation of low-grade from high-grade clear cell renal cell carcinoma. AJR Am J Roentgenol *205(2)*: W193-W201, 2015. PMID: 26204307. DOI: 10.2214/AJR.14.13802

Received September 4, 2022
Revised September 19, 2022
Accepted September 21, 2022